# A Strategy to Design Substituted Tetraamino-Phenazine Dyes and Access to an NIR-Absorbing Benzoquinonediimine-Fused Quinoxaline

Tatiana Munteanu, Valérie Mazan, Mourad Elhabiri, Camil Benbouziyane, Gabriel Canard, Denis Jacquemin, Olivier Siri, Simon Pascal

▶ **To cite this version:**

Tatiana Munteanu, Valérie Mazan, Mourad Elhabiri, Camil Benbouziyane, Gabriel Canard, et al.. A Strategy to Design Substituted Tetraamino-Phenazine Dyes and Access to an NIR-Absorbing Benzoquinonediimine-Fused Quinoxaline. Organic Letters, In press, 10.1021/acs.orglett.3c01251 . hal-04103261

**HAL Id: hal-04103261**
**https://hal.science/hal-04103261**

Submitted on 23 May 2023

**HAL** is a multi-disciplinary open access archive for the deposit and dissemination of scientific research documents, whether they are published or not. The documents may come from teaching and research institutions in France or abroad, or from public or private research centers.

L'archive ouverte pluridisciplinaire **HAL**, est destinée au dépôt et à la diffusion de documents scientifiques de niveau recherche, publiés ou non, émanant des établissements d'enseignement et de recherche français ou étrangers, des laboratoires publics ou privés.

# A Strategy to Design Substituted Tetraamino-Phenazine Dyes and Access to an NIR-Absorbing Benzoquinonediimine-Fused Quinoxaline

Tatiana Munteanu,[a] Valérie Mazan,[b] Mourad Elhabiri,[b] Camil Benbouziyane,[a] Gabriel Canard,[a] Denis Jacquemin,[c,d,*] Olivier Siri,[a,*] Simon Pascal[a,c,*]

[a] *Aix Marseille Univ, CNRS, CINaM, UMR 7325, Marseille, France. E-mail: simon.pascal@cnrs.fr*

[b] *Université de Strasbourg, Université de Haute-Alsace, CNRS, LIMA, UMR 7042, Equipe Chimie Bioorganique et Médicinale, ECPM, Strasbourg, France*

[c] *Université de Nantes, CEISAM, UMR 6230, CNRS, Nantes, France*

[d] *Institut Universitaire de France (IUF), Paris, France*

The straightforward access to N- or C-substituted dinitro-tetraamino-phenazines (**P1-P5**) is enabled in oxidative conditions via two intermolecular C-N bonds formation from accessible 5-nitrobenzene-1,2,4-triamine precursors. The photophysical studies revealed green absorbing and orange-red emitting dyes, with enhanced fluorescence in the solid state. Further reduction of the nitro functions led to the isolation of a benzoquinonediimine-fused quinoxaline (**P6**), which undergoes diprotonation to form a dicationic coupled trimethine dye absorbing beyond 800 nm

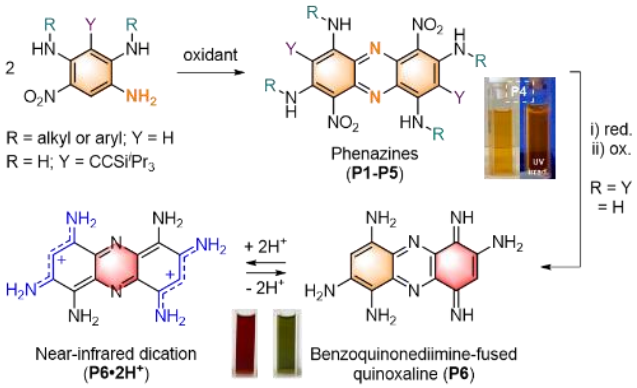


Phenazines are tricyclic dibenzannulated heterocycles containing a central pyrazine core, well-known as naturally occurring substances, biologically active species and dyestuffs (*e.g.* safranine, neutral red).[1–6] Beyond being popular chromophores, their unique optical and electrochemical properties allowed for their use as chemosensors[7,8] or photocatalysts for photopolymerization or cross-coupling reactions.[9–11] In organic electronics, phenazines have demonstrated their potential as low bandgap semiconductors in solar cells,[12,13] and as electro-active compounds in batteries.[14,15] They have also found a particular interest for the elaboration of organic light-emitting diodes (OLEDs), notably due to the rigidity and electron-withdrawing character of the phenazine core, which is beneficial for designing thermally activated delayed fluorescent dyes,[16] as exemplified with the recent report of sterically hindered tetrabenzophenazine-phenoxazines that afforded efficient orange-red OLEDs.[17] Furthermore, the straightforward synthesis of simple phenazines through polycondensation reactions enables the preparation of various π-extended planar chromophores derived from azaacenes, and this motif can be found in many polyaromatic heterocyclic nanographenes,[18] two-dimensional conjugated macrocycles,[19] 3D porous architectures,[20–22] as well as helicoidal derivatives.[23,24]

Seminal strategies to access phenazine dyes are based on the condensation of nitrobenzene and aniline derivatives at high temperature in the presence of base (Wohl-Aue procedure), the ring enlargement of benzofuran-1-oxide (Beirut reaction) and the condensation of 1,2-diaminobenzenes with various diones or *o*-benzoquinones.[25] Other notable approaches rely on the reaction of *o*-aminobenzophenones and cyclohexanones,[26] or on several catalytic processes including straightforward metal-catalyzed intramolecular cyclization or N-arylation.[27] Interestingly, a handful of works report the formation of phenazines *via* the intermolecular formation of C-N bonds in *ortho* position between two electron-rich aromatic amines.[28] Such reaction, particularly relevant for the present contribution, can occur in the presence of an oxidant such as dioxygen, potassium dioxide or 2,3-dichloro-5,6-dicyano-*p*-benzoquinone (DDQ) to form extended phenazines from amino-derivatives of naphthalene, carbazole or anthracene.[29–32] These protocols principally afford mono- to tetra-substituted phenazines, the principal examples of per-substituted derivatives being the tetrabenzo[*a*,*c*,*h*,*j*]phenazines.[6,25]

Herein we describe a straightforward synthetic approach to access N- or C-substituted dinitro-tetraamino-phenazines *via* the intermolecular C-N bonds formation between two 5-nitrobenzene-1,2,4-triamine precursors (self-condensation), obtained through a controlled mono-reduction protocol. The new phenazines **P1-P5** (Scheme 1) feature four amine moieties (positions 1,3,6,8) and two nitro groups (positions 4,9), and their structures were varied *via* the introduction of N-substituents or ethynyl functions (positions 2,7). We investigated the impact of such modifications on their redox and optical properties, including their solid-state enhanced emission. Moreover, the reduction of the nitro functions borne by the phenazine **P5** led to a unique benzoquinonediimine-fused quinoxaline **P6** absorbing in the near-infrared (NIR) upon diprotonation, due to the generation of two cationic coupled trimethines.[33]

**Scheme 1. Synthesis of Phenazines P1-P5**

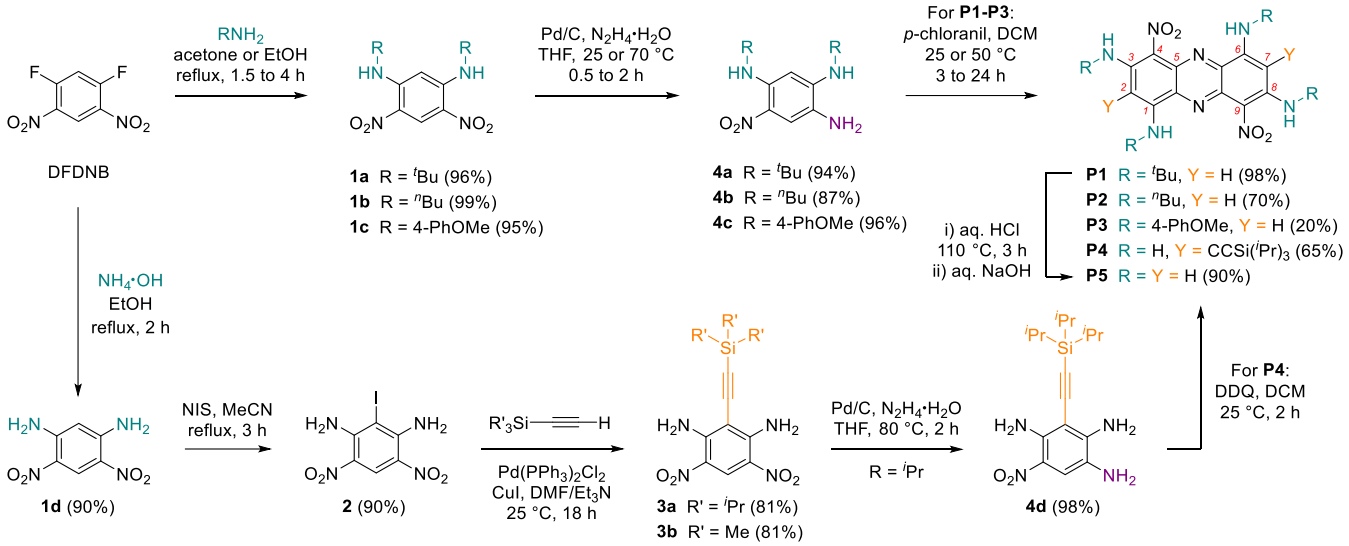


The three-step synthesis of phenazines **P1-P3** starts from 1,5-difluoro-2,4-dinitrobenzene that undergoes nucleophilic aromatic substitution with primary aryl- or alkylamines to readily afford **1a-c** (≥95%). Compound **1d** is prepared in aqueous ammonia and its halogenation using *N*-iodosuccinimide provides compound **2** with 90% yield. The Sonogashira cross-coupling between **2** and ethynyltriisopropylsilane is carried out in the presence of catalytic amounts of Pd(II) and Cu(I) complexes, to give the intermediate **3a** with 81% yield. Prior to this synthesis, conditions were optimized with the less costly ethynyltrimethylsilane and showed that the reaction at room temperature using *N*,*N*-dimethylformamide as solvent leads to the highest yield of **3b** (Table S1). Interestingly, the selective reduction of only one nitro function of **1a-c** or **3a** is efficiently performed with hydrazine in the presence of 5 mol% of Pd/C in up to 2 hours in tetrahydrofuran (THF). Such reaction was previously reported using Raney-Nickel but provided inextricable mixtures of mono- and di-reduced products.[34] Molecules **4a-d** are obtained in excellent yields (87-98%), without forming the totally reduced tetraaminobenzene species that are commonly obtained under similar conditions when ethanol is used as solvent instead of THF,[35] or when other reducing agents such as tin chloride or iron are used.[36,37]

Compound **4b** was used to screen the conditions to form **P2** and designated *p*-chloranil (2 equiv.) as the best oxidizing agent to achieve the highest yield (see Table S2). Increasing the amount of oxidant or changing it to DDQ, magic blue or ferrocenium salt decreases the yield of **P2** formation. For **P3**, the reaction process is complicated by the lower solubility of the starting compound **4c**. While the use of highly polar solvents is ineffective to improve the formation of **P3**, it was possible to increase the yield from 5 to 20% by changing the solvent from dichloromethane (DCM) to chloroform and performing the reaction at 50 °C. Surprisingly, when using more equivalents of oxidant, and especially in the case of magic blue, a benzotriazole derivative was isolated as the major product (see **BT** in Scheme S2 and SI). Several comparable synthesis of benzobistriazole derivatives were previously achieved *via* the diazotation of tetraaminobenzene derivatives in presence of sodium nitrite,[38] suggesting that, in our case, the formation of this unexpected compound is presumably due to the decomposition of a portion of **4b**, acting as a source of nitrogen atoms.

Removal of the *tert*-butyl groups in **P1** was achieved by heating the compound to 110 °C in acidic medium, affording the unsubstituted phenazine **P5** with 90% yield. Unlike compounds **P1-P4**, which were purified by flash column chromatography, the low solubility of **P5** allowed the removal of the impurities by simply washing the precipitate with water and DCM. Attempts to reduce the nitro functions of the phenazines **P1-P4** were carried out using Pd/C with $H_2$ or $N_2H_4$, $SnCl_2$, Fe or Zn in acidic medium. These conditions led to either the recovery of starting material or inextricable mixtures containing unidentified species. However, reduction of **P5** using Pd/C and $H_2$ followed by an aerobic workup gave **P6** in 77% yield (Scheme 2). The compound was characterized by HRMS, showing a molecular peak at $m/z$ = 269.1256 ($m/z_{theo}$ = 269.1258) corresponding to [**P6**+H$^+$]. The $^1$H NMR of **P6** revealed an unsymmetrical structure with two singlets corresponding to the two CH protons at 6.52 and 6.26 ppm, two singlets imine protons at 12.05 and 6.37 ppm, and four broad singlets corresponding to the amine functions (Figure S31). The structure depicted in Scheme 2 is also the most stable tautomer obtained by DFT calculations (*vide infra*). In acidic medium, the $^1$H NMR of **P6** shows two equivalent CH protons at 6.33 ppm (Figure S34), suggesting a symmetrical structure corresponding to the dicationic species **P6**•**2H**$^{2+}$, which could be isolated with 83% yield.

**Scheme 2. Formation and protonation states of P6.**

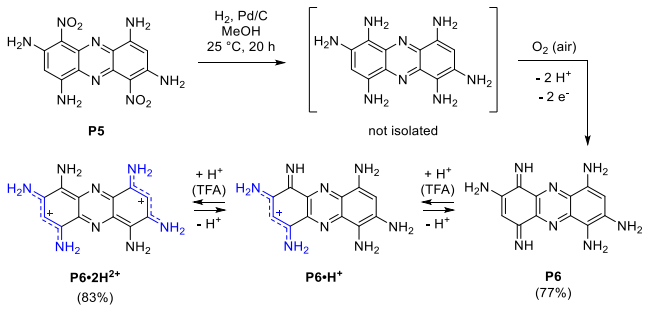


The slow evaporation of a **P4** solution in DCM afforded single crystals (Figure 1). The bond length analysis confirms a centrosymmetric structure with aromatic rings, and shows an intramolecular hydrogen bond between one H atom of the

amine substituent in position 3 and one O atom of the nitro function in position 4.

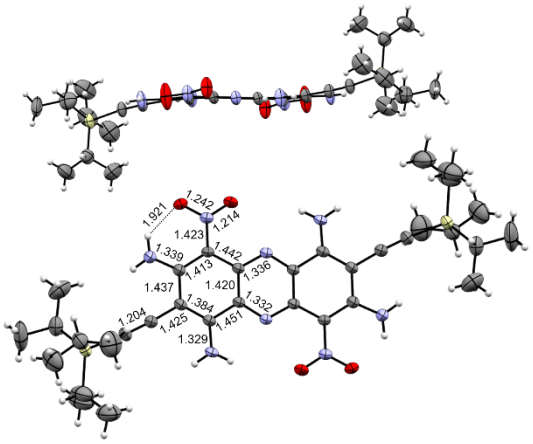


**Figure 1.** Single crystal structure of **P4**: side and top views with distances indicated in Å. Anisotropic displacement ellipsoids plot at the 50% probability level.

The electrochemical properties of **P1-P4** were investigated by cyclic voltammetry in DCM and revealed irreversible redox processes (Table S6 and Figure S74). Both phenazines **P1** and **P2** exhibit similar electrochemical signatures with first reduction and oxidation waves at *ca*. -0.88 and 0.56 V *vs.* $Fc/Fc^+$, respectively. Replacing alkyl N-substituents with electron-donating *p*-methoxyphenyl groups in **P3** mainly impacts the reduction process that is shifted to -1.19 V. In contrast, the triisopropylsilylacetylenes on positions 2,7 of **P4** facilitate the reduction, with a wave at -0.62 V and shifts the oxidation to a more anodic potential at 1.02 V.

The phenazines **P1-P5** display significantly redshifted absorptions compared to the triamine precursors **4a-d** due to their π-extended tricyclic structure (Figure 2 and Figure S75). Their lowest energy absorption bands are found in the green region, peaking at ~510 nm with an extinction coefficient of *ca*. 10,000 $M^{-1}cm^{-1}$, except for N-aryl substituted **P3**, for which the absorption maximum is slightly redshifted to 533 nm (Table S6). Interestingly, the four phenazines exhibit emission in the orange-red with maxima at *ca.* 580-600 nm for **P1**, **P2** and **P4**, and 650 nm for **P3**. The fluorescence quantum yields (Φ) are estimated <0.1%, except for **P4** (Φ=0.45%). The weak fluorescence is typical of nitro-substituted dyes, which generally promote deexcitation *via* various non-radiative pathways including intersystem crossing,[39] and calculations indeed predict small S-T gaps in **P1-P4**, though with relatively small SOC couplings (see the SI). However, the latter was ruled out through measurements in degassed 2-methyltetrahydrofuran at 77 K, which did not reveal the presence of triplet state emission in the spectral window studied (Figure S77). Interestingly, solid-state fluorescence was detected from the powders of phenazines **P1**, **P2**, and **P4**. Thin films of these compounds were thus prepared by drop-casting on glass substrates and revealed emissions with comparable maxima but higher intensity compared to solution (Figure S78). This emission enhancement was studied in $THF/H_2O$ mixtures allowing for the progressive precipitation of **P1**. From THF to a 4:3 $THF/H_2O$ mixture, the absorption features remain unchanged and the weak emission is maintained, with Φ≤0.2% (Figure S79 and Table S7). For higher water content, the absorption is markedly broadened and lowered due to the precipitation of the dye. However, the Φ value is increased to 10.4% in a 2:8 $THF/H_2O$ mixture, as a result of the aggregated state of **P1** decreasing nonradiative deactivation.

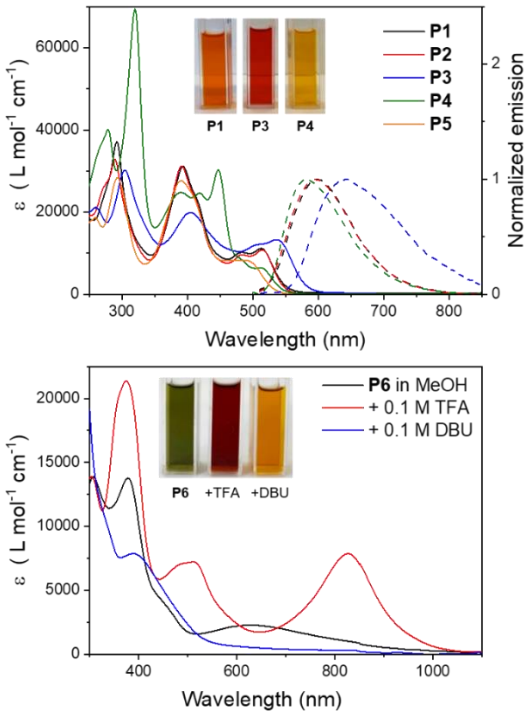


**Figure 2.** Top: electronic absorption (plain lines) and emission (dashed lines) spectra of **P1-P4** in DCM and absorption of **P5** in DMSO. Bottom: Electronic absorption spectra of **P6** in MeOH without or with the presence of 0.1 M 1,8-diazabicyclo[5.4.0]undec-7-ene (DBU) or 0.1 M trifluoroacetic acid (TFA).

The absorption spectrum of **P6** in methanol solution displayed in Figure 2 shows a broad band centered at 642 nm, which is blueshifted to *ca*. 600 nm in DMSO (Figure S76). On the one hand, in the presence of DBU, the band is blueshifted to the UV region, hinting at deprotonation of the solvated species, whereas, on the other hand, in the presence of TFA, an intense band appears in the NIR at *ca.* 830 nm. Such large redshift can be attributed to the formation of coupled cationic trimethine cyanines (Scheme 2). To determine the protonation states of **P6** and fully understand its acid-base properties, the pH-dependent absorption was investigated and compared to theoretical calculations.

The absorption spectra of fresh **P6** solutions recorded at different pH values in a $CH_3OH/H_2O$ mixture (8:2 *w/w*) were first found to agree with those measured in pure $CH_3OH$ (Figure S80). While these solvent conditions ensured a good solubility of **P6**, a slow kinetics most likely related to hydrolysis of the iminium functions was found with fading of the visible-NIR absorptions of **P6** over time (Figures S75-76). This is consistent with *p*-benzoquinone mono- and diimine related compounds described to undergo rapid hydrolysis in water.[40] Based on these observations, absorption spectrophotometric titrations *vs.* pH were performed to cover a wide pH range and prevent as much as possible hydrolysis reactions (Figures S77-79). Two protonation values attributed to the imine functions ($pK_{a1}$= 2.5±0.7 and $pK_{a2}$= 10.1±0.1) were determined and are characterized by absorption in the visible-NIR region. The difference in the $pK_a$ values can be explained by the strong electrostatic repulsion within the dicationic species. These data are consistent with phenylene blue (indamine),[41] which has a $pK_a$ of 7.55 and whose protonation induces the formation of a cationic species with an absorption maximum shifting from 484 to 672 nm. Finally, under very acidic conditions, the **P6•2H$^{2+}$** species was shown to undergo

further protonations, characterized by the loss of the NIR absorptions (Figure S86).

We have then used TD-DFT to model **P1-P4** and **P6** (see SI for details). The electron density difference (EDD) plots for the lowest transition of **P1** in Figure 3 indicates a clear π-π* character. Interestingly, the lateral amino and nitro groups have a rather small role in the transition that is centered on the phenazine core, its central pyrazine moiety acting as a strong accepting unit (mostly in red). The topology of the transitions remains similar in both **P3** and **P4**, *i.e.*, the side groups attached at positions 2 and 7 have trifling influence on the lowest transition, consistent with the very similar $\lambda_{max}$ measured.

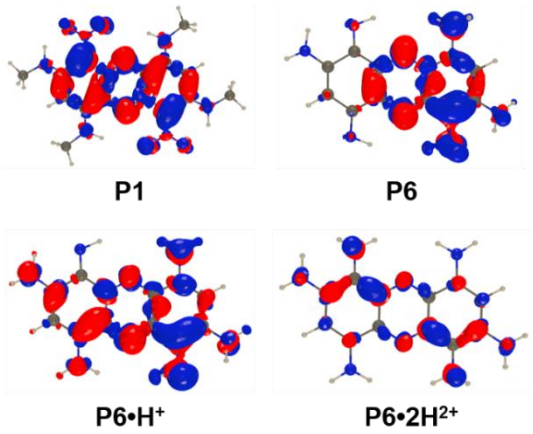


**Figure 3.** EDD plots of the lowest singlet transition of selected dyes. The blue and red lobes represent decrease and increase of density upon absorption, respectively.

For **P6**, we have performed a thorough tautomer search for the neutral, mono- and diprotonated species, and in all three forms, one tautomeric form clearly emerged as most stable (Scheme 2), the other tautomers being less stabilized by at least 5 kcal.mol$^{-1}$. Protonation of the central pyrazine rather than side amines clearly leads to less stable species (see SI). For the stable forms of neutral and protonated **P6**, we modelled the excited states using calculations including CC2 corrections[42] as well as cLR$^2$ solvation corrections.[43] For the lowest transition, this yields 566 nm (*f*=0.070) for non-protonated **P6**, the transition inducing an obviously strong charge-transfer (CT) from the diamino-phenyl towards the pyrazine moiety (Figure 3), corresponding to the very broad weak band at 642 nm experimentally (Figure 2). After a single protonation, theory foresees transitions at 703 nm (*f*=0.019) and 622 nm (*f*=0.146), both involving CT (see Figure 3 for the former), which does not fit well the experimental observation of a band redshifted by 186 nm and much more intense upon TFA addition. In contrast, the diprotonated **P6•2H$^{2+}$** presents a calculated vertical transition that is both strongly redshifted (+166 nm) and much more intense: 732 nm (*f*=0.363), clearly fitting the experimental observations. Strikingly, this low-lying excited state presents a totally different topology. An analysis of the DFT bond lengths in **P6•2H$^{2+}$** indicates that the structure presents two trimethine units with negligible bond length alternation, as represented in Scheme 2.

In conclusion, a new synthetic approach allowed the preparation of functionalized tetraamino-phenazines in at least three steps. These dyes present photophysical properties in the visible region and hold potential for future applications in material sciences or as platforms to reach π-extended fused chromophores. Finally, the characterization of an intriguing fused benzoquinonedimine-quinoxaline and its protonated forms showing NIR absorption further stimulates the research on overlooked coupled polymethine dyes.

## Supporting Information

Experimental protocols, single-crystal X-ray, NMR spectra, computational, and spectroscopic characterization data (PDF).

## Single-crystal X-ray

CCDC 2256019 (compound **3b**), 2256023 (compound **P1**) and 2256032 (compound **P4**), contain the supplementary crystallographic data for this paper. These data can be obtained free of charge via www.ccdc.cam.ac.uk/data_request/cif, or by emailing data_request@ccdc.cam.ac.uk, or by contacting The Cambridge Crystallographic Data Centre, 12 Union Road, Cambridge CB2 1EZ, UK; fax: +44 1223 336033.

## ACKNOWLEDGMENT

We thank the *Région SUD* and the *Agence Nationale de la Recherche* for the attribution of grants in the frame of the *MALDI* project and the SOCOOL project (ANR-20-CE07-0024), respectively. We acknowledge Michel Giorgi and Valérie Monnier (*Spectropole*, Aix-Marseille Univ) for the X-ray and HRMS analyses, respectively. D.J. is indebted to the CCIPL/GliciD center for computational time.

## REFERENCES

(1) Turner, J. M.; Messenger, A. J. Occurrence, Biochemistry and Physiology of Phenazine Pigment Production. Adv. Microb. Physiol. **1986**, 27, 211–275. https://doi.org/10.1016/S0065-2911(08)60306-9.

(2) Beifuss, U.; Tietze, M. Methanophenazine and Other Natural Biologically Active Phenazines. In *Natural Products Synthesis II: Targets, Methods, Concepts*; Mulzer, J., Ed.; Springer Berlin Heidelberg: Berlin, Heidelberg, 2005; pp 77–113. https://doi.org/10.1007/b96889.

(3) Schiessl, K. T.; Hu, F.; Jo, J.; Nazia, S. Z.; Wang, B.; Price-Whelan, A.; Min, W.; Dietrich, L. E. P. Phenazine Production Promotes Antibiotic Tolerance and Metabolic Heterogeneity in Pseudomonas Aeruginosa Biofilms. *Nat. Commun.* **2019**, *10* (1), 762. https://doi.org/10.1038/s41467-019-08733-w.

(4) Kohatsu, H.; Kamo, S.; Tomoshige, S.; Kuramochi, K. Total Syntheses of Pyocyanin, Lavanducyanin, and Marinocyanins A and B. *Org. Lett.* **2019**, *21* (18), 7311–7314. https://doi.org/10.1021/acs.orglett.9b02601.

(5) Lee, H.-S.; Kang, J. S.; Cho, D.-Y.; Choi, D.-K.; Shin, H. J. Isolation, Structure Determination, and Semisynthesis of Diphenazine Compounds from a Deep-Sea-Derived Strain of the Fungus Cystobasidium Laryngis and Their Biological Activities. *J. Nat. Prod.* **2022**, *85* (4), 857–865. https://doi.org/10.1021/acs.jnatprod.1c00985.

(6) Che, Y.-X.; Qi, X.-N.; Lin, Q.; Yao, H.; Qu, W.-J.; Shi, B.; Zhang, Y.-M.; Wei, T.-B. Design Strategies and Applications of Novel Functionalized Phenazine Derivatives: A Review. *J. Mater. Chem. C* **2022**, *10* (31), 11119–11174. https://doi.org/10.1039/D2TC02085H.

(7) Banerjee, S. Phenazines as Chemosensors of Solution Analytes and as Sensitizers in Organic Photovoltaics. *ARKIVOC* **2016**, *2016* (1), 82–110. https://doi.org/10.3998/ark.5550190.p009.347.

(8) Xiao-Ni, Q.; Dang, L.-R.; Qu, W.-J.; Zhang, Y.-M.; Yao, H.; Lin, Q.; Wei, T.-B. Phenazine Derivatives for Optical Sensing: A Review. *J. Mater. Chem. C* **2020**, *8* (33), 11308–11339. https://doi.org/10.1039/D0TC01401J.

(9) Cole, J. P.; Federico, C. R.; Lim, C.-H.; Miyake, G. M. Photoinduced Organocatalyzed Atom Transfer Radical Polymerization Using Low Ppm Catalyst Loading. *Macromolecules* **2019**, *52* (2), 747–754. https://doi.org/10.1021/acs.macromol.8b02688.

(10) Deol, H.; Singh, G.; Kumar, M.; Bhalla, V. Phenazine-Based Donor Acceptor Systems as Organic Photocatalysts for "Metal-Free" C–N/C–C Cross-Coupling. *J. Org. Chem.* **2020**, *85* (17), 11080–11093. https://doi.org/10.1021/acs.joc.9b03407.

(11) Bobo, M. V.; Kuchta, J. J.; Vannucci, A. K. Recent Advancements in the Development of Molecular Organic Photocatalysts. *Org. Biomol. Chem.* **2021**, *19* (22), 4816–4834. https://doi.org/10.1039/D1OB00396H.

(12) Mastalerz, M.; Fischer, V.; Ma, C.-Q.; Janssen, R. A. J.; Bäuerle, P. Conjugated Oligothienyl Dendrimers Based on a Pyrazino[2,3-g]Quinoxaline Core. *Org. Lett.* **2009**, *11* (20), 4500–4503. https://doi.org/10.1021/ol9015546.

(13) Li, Y.; Meng, B.; Tong, H.; Xie, Z.; Wang, L. A Chlorinated Phenazine-Based Donor–Acceptor Copolymer with Enhanced Photovoltaic Performance. *Polym. Chem.* **2014**, *5* (6), 1848–1851. https://doi.org/10.1039/C3PY01436C.

(14) Pang, S.; Wang, X.; Wang, P.; Ji, Y. Biomimetic Amino Acid Functionalized Phenazine Flow Batteries with Long Lifetime at Near-Neutral PH. *Angew. Chem. Int. Ed.* **2021**, *60* (10), 5289–5298. https://doi.org/10.1002/anie.202014610.

(15) Tie, Z.; Deng, S.; Cao, H.; Yao, M.; Niu, Z.; Chen, J. A Symmetric All-Organic Proton Battery in Mild Electrolyte. *Angew. Chem. Int. Ed.* **2022**, *61* (8), e202115180. https://doi.org/10.1002/anie.202115180.

(16) Xiao, Y.; Wang, H.; Xie, Z.; Shen, M.; Huang, R.; Miao, Y.; Liu, G.; Yu, T.; Huang, W. NIR TADF Emitters and OLEDs: Challenges, Progress, and Perspectives. *Chem. Sci.* **2022**, *13* (31), 8906–8923. https://doi.org/10.1039/D2SC02201J.

(17) Balijapalli, U.; Lee, Y.-T.; Karunathilaka, B. S. B.; Tumen-Ulzii, G.; Auffray, M.; Tsuchiya, Y.; Nakanotani, H.; Adachi, C. Tetrabenzo[a,c]Phenazine Backbone for Highly Efficient Orange–Red Thermally Activated Delayed Fluorescence with Completely Horizontal Molecular Orientation. *Angew. Chem. Int. Ed.* **2021**, *60* (35), 19364–19373. https://doi.org/10.1002/anie.202106570.

(18) Borissov, A.; Maurya, Y. K.; Moshniaha, L.; Wong, W.-S.; Żyła-Karwowska, M.; Stępień, M. Recent Advances in Heterocyclic Nanographenes and Other Polycyclic Heteroaromatic Compounds. *Chem. Rev.* **2022**, *122* (1), 565–788. https://doi.org/10.1021/acs.chemrev.1c00449.

(19) Marco, A. B.; Cortizo-Lacalle, D.; Perez-Miqueo, I.; Valenti, G.; Boni, A.; Plas, J.; Strutyński, K.; De Feyter, S.; Paolucci, F.; Montes, M.; Khlobystov, A. N.; Melle-Franco, M.; Mateo-Alonso, A. Twisted Aromatic Frameworks: Readily Exfoliable and Solution-Processable Two-Dimensional Conjugated Microporous Polymers. *Angew. Chem. Int. Ed.* **2017**, *56* (24), 6946–6951. https://doi.org/10.1002/anie.201700271.

(20) Kohl, B.; Rominger, F.; Mastalerz, M. Rigid π-Extended Triptycenes via a Hexaketone Precursor. *Org. Lett.* **2014**, *16* (3), 704–707. https://doi.org/10.1021/ol403383y.

(21) Hu, B.-L.; An, C.; Wagner, M.; Ivanova, G.; Ivanova, A.; Baumgarten, M. Three-Dimensional Pyrene-Fused N-Heteroacenes. *J. Am. Chem. Soc.* **2019**, *141* (13), 5130–5134. https://doi.org/10.1021/jacs.9b01082.

(22) Lauer, J. C.; Kohl, B.; Braun, F.; Rominger, F.; Mastalerz, M. A Hexagonal Shape-Persistent Nanobelt of Elongated Rhombic Symmetry with Orthogonal π-Planes by a One-Pot Reaction. *Eur. J. Org. Chem.* **2022**, *2022* (8), e202101317. https://doi.org/10.1002/ejoc.202101317.

(23) Jakubec, M.; Hansen-Troøyen, S.; Císařová, I.; Sýkora, J.; Storch, J. Photochemical Oxidation Specific to Distorted Aromatic Amines Providing Ortho-Diketones. *Org. Lett.* **2020**, *22* (10), 3905–3910. https://doi.org/10.1021/acs.orglett.0c01190.

(24) Chen, F.; Melle-Franco, M.; Mateo-Alonso, A. Planar and Helical Dinaphthophenazines. *J. Org. Chem.* **2022**, *87* (12), 7635–7642. https://doi.org/10.1021/acs.joc.2c00129.

(25) Chaudhary, A.; Khurana, J. M. Synthetic Routes for Phenazines: An Overview. *Res. Chem. Intermed.* **2018**, *44* (2), 1045–1083. https://doi.org/10.1007/s11164-017-3152-8.

(26) Xiao, Y.; Hu, W.; Sun, S.; Yu, J.-T.; Cheng, J. Recent Advances in the Synthesis of Acridines and Phenazines. *Synlett* **2019**, *30* (19), 2113–2122.

(27) Emoto, T.; Kubosaki, N.; Yamagiwa, Y.; Kamikawa, T. A New Route to Phenazines. *Tetrahedron Lett.* **2000**, *41* (3), 355–358. https://doi.org/10.1016/S0040-4039(99)02061-4.

(28) Hiroto, S. Synthesis of π-Functional Molecules through Oxidation of Aromatic Amines. *Chem. – Asian J.* **2019**, *14* (15), 2514–2523. https://doi.org/10.1002/asia.201900213.

(29) Crank, G.; Makin, M. I. H. Organic Chemistry of Superoxide. II Oxidation of β-Naphthylamine - Possible Involvement of the Hydroxyl Radical. *Tetrahedron Lett.* **1983**, *24* (30), 3159–3160. https://doi.org/10.1016/S0040-4039(00)88122-8.

(30) Piechowska, J.; Virkki, K.; Sadowski, B.; Lemmetyinen, H.; Tkachenko, N. V.; Gryko, D. T. Excited State Intramolecular Proton Transfer in π-Expanded Phenazine-Derived Phenols. *J. Phys. Chem. A* **2014**, *118* (1), 144–151. https://doi.org/10.1021/jp411395c.

(31) Kosugi, Y.; Itoho, K.; Okazaki, H.; Yanai, T. Unexpected Formation of Dibenzo[a,h]Phenazine in the Reaction between 1-Naphthyliminodimagnesium Dibromide and 1-Nitronaphthalene. *J. Org. Chem.* **1995**, *60* (17), 5690–5692. https://doi.org/10.1021/jo00122a063.

(32) Nagasaki, J.; Hiroto, S.; Shinokubo, H. π-Extended Dihydrophenazines with Three-State NIR Electrochromism Involving Large Conformational Changes. *Chem. – Asian J.* **2017**, *12* (17), 2311–2317. https://doi.org/10.1002/asia.201700840.

(33) Dähne, S.; Leupold, D. Coupling Principles in Organic Dyes. *Angew. Chem. Int. Ed. Engl.* **1966**, *5* (12), 984–993. https://doi.org/10.1002/anie.196609841.

(34) Gampe, D. M.; Kaufmann, M.; Jakobi, D.; Sachse, T.; Presselt, M.; Beckert, R.; Görls, H. Stable and Easily Accessible Functional Dyes: Dihydrotetraazaanthracenes as Versatile Precursors for Higher Acenes. *Chem. – Eur. J.* **2015**, *21* (20), 7571–7581. https://doi.org/10.1002/chem.201500230.

(35) Pascal, S.; Lavaud, L.; Azarias, C.; Canard, G.; Giorgi, M.; Jacquemin, D.; Siri, O. Controlling the Canonical/Zwitterionic Balance through Intramolecular Proton Transfer: A Strategy for Vapochromism. *Mater. Chem. Front.* **2018**, *2* (9), 1618–1625. https://doi.org/10.1039/C8QM00171E.

(36) Lavaud, L.; Chen, Z.; Elhabiri, M.; Jacquemin, D.; Canard, G.; Siri, O. Di- vs. Tetra-Substituted Quinonediimines: A Drastic Effect on Coordination Chemistry. *Dalton Trans.* **2017**, *46* (38), 12794–12803. https://doi.org/10.1039/C7DT01884C.

(37) Lavaud, L.; Azarias, C.; Canard, G.; Pascal, S.; Galiana, J.; Giorgi, M.; Chen, Z.; Jacquemin, D.; Siri, O. Fused Bis-Azacalixphyrin That Reaches NIR-II Absorptions. *Chem. Commun.* **2020**, *56* (6), 896–899. https://doi.org/10.1039/C9CC09021E.

(38) Tomé, A. C. Product Class 13: 1,2,3-Triazoles. In *Category 2, Hetarenes and Related Ring Systems*; Science of Synthesis; Georg Thieme Verlag KG: Stuttgart, 2004; Vol. 13. https://doi.org/10.1055/sos-SD-013-00626.

(39) Poronik, Y. M.; Sadowski, B.; Szychta, K.; Quina, F. H.; Vullev, V. I.; Gryko, D. T. Revisiting the Non-Fluorescence of Nitroaromatics: Presumption versus Reality. *J. Mater. Chem. C* **2022**, *10* (8), 2870–2904. https://doi.org/10.1039/D1TC05423F.

(40) Corbett, J. F. Benzoquinoneimines. II. Hydrolysis of p-Benzoquinone Monoimine and p-Benzoquinone Di-Imine. *J. Chem. Soc. B* **1969**, 213–216. https://doi.org/10.1039/J29690000213.

(41) Corbett, J. F.; Gamson, E. P. Benzoquinone Imines. Part XI. Mechanism and Kinetics of the Reaction of p-Benzoquinone Di-Imines with Aniline and Its Derivatives. *J. Chem. Soc. Perkin Trans. 2* **1972**, No. 11, 1531–1537. https://doi.org/10.1039/P29720001531.

(42) Christiansen, O.; Koch, H.; Jørgensen, P. The Second-Order Approximate Coupled Cluster Singles and Doubles Model CC2. *Chem. Phys. Lett.* **1995**, *243* (5), 409–418. https://doi.org/10.1016/0009-2614(95)00841-Q.

(43) Guido, C. A.; Chrayteh, A.; Scalmani, G.; Mennucci, B.; Jacquemin, D. Simple Protocol for Capturing Both Linear-Response and State-Specific Effects in Excited-State Calculations with Continuum Solvation Models. *J. Chem. Theory Comput.* **2021**, *17* (8), 5155–5164. https://doi.org/10.1021/acs.jctc.1c00490.